

# Buried Unexploded Ordnance Detection Using Energy-Based Features of Ground Penetrating Radar Signals

**Nipon Theera-Umpon**

Department of Electrical Engineering,  
Faculty of Engineering, Chiang Mai University,  
Chiang Mai 50200 Thailand  
E-mail: nipon@ieee.org

## Abstract

Buried unexploded ordnance (UXO) and land mines are considered a serious threat to the world, particularly during the return of civilians to contaminated areas. Consequently, humanitarian demining is required before the civilian returning process can proceed. Several humanitarian demining projects were established by organizations and governments including the United Nations, the Royal Thai government, the U.S. government, the Japanese government, etc. In this research we propose a new technique to discriminate UXO from non-UXO targets based on the energy of returning ground penetrating radar (GPR) signals in the time-domain. In the experiments we analyze the GPR data sets collected by Battelle company and the Ohio State University from the Jefferson Proving Ground (JPG), U.S.A. The results are evaluated in terms of Receiver Operating Characteristic (ROC) curves that provide information of the UXO detection ability of our technique. The ROC curves show that our proposed technique performs better than a traditional detection technique based on energy only. In addition, both techniques yield better results than the situation in which no technique is applied (no discrimination ability.)

**Keywords:** Humanitarian Demining, Unexploded Ordnance Detection, Ground Penetrating Radar, Probability of Detection, Probability of False Alarms, ROC Curve

## 1. Introduction

### 1.1 Buried UXO/Land Mine Problem

Buried unexploded ordnance (UXO) and land mines pose serious problems all over the world [1]. It is estimated that there are between 60 and 100 million of them buried around the world and that someone is killed or injured by them every 20 minutes [2]. The main problem arises when pieces of land are returned to civilians after wars. Even after the efforts to clear those contaminated sites, several areas were handed over to civilians without adequate UXO and land mines clearance [3].

During war time, these military weapons are used intentionally to kill or injure military personnel on the opposite side. To make this more serious, during the post-war period, these weapons still cause humanitarian problems unintentionally. Besides the problems of the

injuries and casualties of civilians from UXO and land mines, the fear of contamination also prevents civilians from using to use the lands. Therefore, this problem affects the whole world in many ways including public safety, society, environment, and economy.

### 1.2 Thailand's Role in Humanitarian Demining

There is no exception for Thailand in the UXO/land mine problem. A significant portion, almost 800 square kilometers, of Thai territory is mined. These areas stretch over 18 border provinces in the northern, northeastern, southern, and western parts of Thailand. These UXO and land mines result in a condition in which a Thai innocent victim dies or is injured in an explosion every three days.

In 1997, the Royal Thai Government signed the Convention on the Prohibition of the Use,

Stockpiling, Production, and Transfer of Anti-Personnel Mines in Ottawa. Thailand then deposited its ratification instrument at the United Nations in 1998 as the first nation in Southeast Asia to do so. In the same year, the Royal Thai Government formed the National Committee on Anti-Personnel Mine Management which in turn formed the Thailand Mine Action Center or TMAC operating under the royal patronage of Her Royal Highness Princess Galyani Vadhana Krom Lung Naradhiwas Rajnagarindra [4].

### 1.3 UXO/Land mine clearance efforts

During the clearance effort, when an operator of a UXO/land mine detection system encounters a location that the system alarms, he would guess that the location is mined and dig up the ground. However, most of the time they are false alarms, i.e., those locations contain some other objects, other than UXO or land mines, e.g., bottle caps, soda cans, fragments from exploded ordnance, etc. A detection system that can specify targets more correctly is preferred. The reduction of false alarms cuts the expense and time of the clearance operation.

The most familiar detector is a metal detector. The metal detector-based detection system, however, does not work well in many situations because it identifies every metal object as a target. One of these situations is when the buried object is a metal fragment (like a non-UXO object in this research.) For this reason, there are many efforts to apply ground penetrating radar (GPR) signals in UXO/land mine detection [5]–[18]. GPR-based detection systems work better than the traditional metal detector-based systems in many aspects, especially when the target contains a very small metal content, for example, an M14 antipersonnel land mine or an M19 antitank land mine [1].

In addition, many efforts are also applied to solve the UXO/land mine detection by analyzing GPR data. Many computational tools are applied to this problem, for example, fuzzy systems [7]–[10], hidden Markov model [11], linear prediction [12]–[14], artificial neural networks [15], [16], size-contrast filtering in region-based analysis [17], statistical approach [18], etc. Many researchers also proposed fusion algorithms to fuse data collected from

several sensors or fuse outputs of several algorithms [10, [19]–[21].

This paper is organized as follows: Section 2 describes the brief details of data we use in the experiments. The details of our proposed technique are given in section 3. We show the results and describe how to interpret them in section 4. Section 5 concludes this paper.

## 2. UXO GPR Data Set

In the experiments, we used the GPR data set collected from the Jefferson Proving Ground (JPG), near Madison, Indiana, U.S.A., by Battelle company and the Ohio State University [3], [22]. The data set were collected over four days from September 21 to 24, 1998. This data set is made available to the public by the Unexploded Ordnance Center of Excellence (UXOCOE), Department of Defense, U.S.A.

The UXO characterization system used in the data collection is a manually-operated, surface-towed, ground penetrating radar (GPR). A Hewlett Packard network analyzer (HP8753C) was applied in the radar system to measure multiple frequency responses by sweeping the frequency 2 MHz at a time from 20 MHz to 420 MHz. The bandwidth of 400 MHz provides a depth resolution of 2.5 nanosecond (ns). Therefore, there are 201 responses in each measurement. Additionally, in each measurement, the system antenna was lowered onto the ground surface and then rotated to collect responses for a total of 180 degrees with 10 degree increments. At the end, 18 sets of 201-sample one-dimensional signals were collected. We arrange these signals in the form of images with a size of 201×18. It should be noted that these GPR signals are not real images. We arrange and display them this way to ease visualization.

This data set contains several types of UXO from the Jefferson Proving Ground (JPG) site. Here are some examples of UXO found in this site – High Explosive (HE) with the sizes of 20mm, 76mm and 152mm, Mortar with the sizes of 60mm and 81mm, Armor Piercing (AP) with the size of 90mm, etc [3]. The objects in the non-UXO class in this data set are fragments that are usually scattered all over war zones. Sample GPR images of UXO (20 mm high explosive) and non-UXO (fragment) are shown in Figures 1 and 2, respectively.

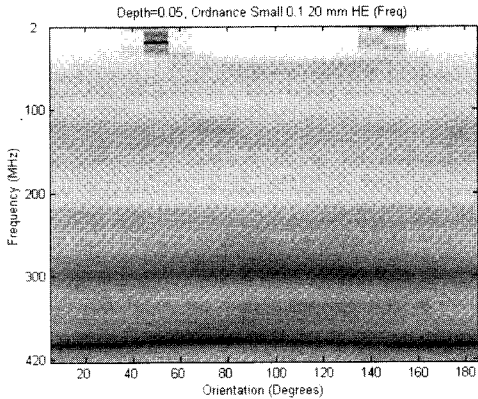


**Figure 1.** Sample GPR image of UXO (20 mm high explosive) in frequency domain.

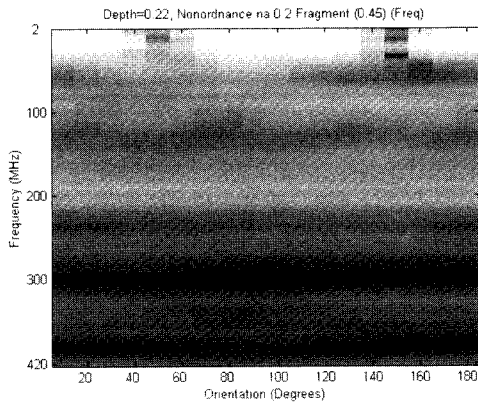


**Figure 2.** Sample GPR image of non-UXO (fragment) in frequency domain.

The target locations on the test site were marked with flags to provide ground truths of the target locations. Each target could be a UXO or non-UXO. The ground truth of the type of each target was also given in the data set. The numbers of UXO and non-UXO collected each day are shown in Table 1.

**TABLE 1**  
**THE NUMBERS OF UXO AND NON-UXO**  
**COLLECTED EACH DAY IN THE DATA SET.**

Object	Day				Total
	1	2	3	4	
UXO	13	17	13	7	50
Non-UXO	27	31	33	18	109

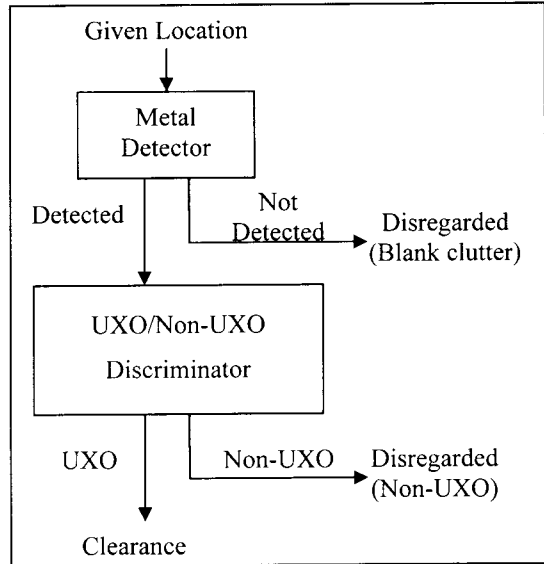


**Figure 3.** An example of UXO detection system.

### 3. Proposed Technique

The goal of this research is to decide whether or not an object in a given GPR image is a buried UXO. The non-UXO objects make this problem much more difficult than the UXO/land mine detection problem in which we try to distinguish blank ground and ground with a buried object. Figure 3 shows one possible UXO detection system. The task of the metal detector is only to find a buried piece of metal. The more difficult task is in the next step – the UXO/Non-UXO discrimination – that is what we are trying to achieve in this research.

#### 3.1 GPR Time-Domain Analysis

Our proposed technique is based on the analysis of GPR images in the time domain. This can be achieved by taking the inverse Fourier transform of a signal in each orientation (each column of GPR images.) The time-domain GPR images of the sample GPR images of UXO and non-UXO shown in Figures 1 and 2 are depicted in Figures 4 and 5, respectively. We can see that it is hard or impossible for a human to tell the difference between the GPR signals of UXO and non-UXO either in the frequency or the time domain. Fortunately, the energy of GPR signals from these two classes of objects are somewhat different, particularly when we select only the underground region that we believe contains useful information.

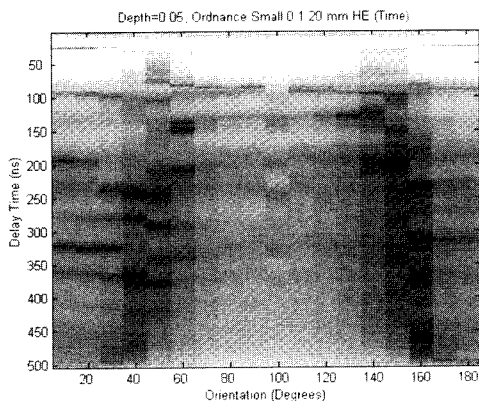


**Figure 4.** Time-domain GPR image of UXO corresponding to the frequency-domain GPR image show in Figure 1.

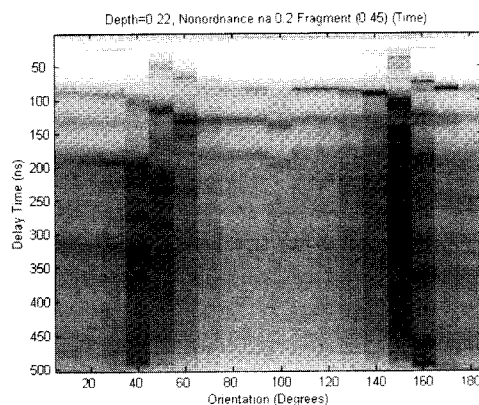


**Figure 5.** Time-domain GPR image of non-UXO corresponding to the frequency-domain GPR image show in Figure 2.

### 3.1.1 Region of Interest Selection

From the time-domain GPR images of the data set, we found that the ground bounces occur around the 7th row (corresponding to a time delay of 17.5 ns which is consistent to what was reported in [3] and [22].) Based on this information, we select the region of interest that contains row 11 to 20 (27.5 to 50 ns) of each time-domain GPR image to eliminate the effects from the ground bounce and eliminate the deep underground area that does not contain objects. This is an advantage of considering GPR signals in time (or spatial) domain in which we can select a useful depth range. This cannot be done easily if the frequency-domain GPR signals are considered.

### 3.1.2 Detector Shifting Problem

One of the difficulties occurring during the data collection process at a given location is the shifting of the detector. The shifting prevents us from associating a signal with the adjacent ones directly. For example, we cannot just subtract one from the other to achieve the change detection. This difficulty always occurs in a hand-held detector unit in which, ideally, we would like to hold the detector unit over the ground at the same height all the time. In the data set used in this research, it is highly possible that the location of the antenna would shift vertically during its 18 orientations.

To solve the vertical shifting problem, we consider one of the Fourier transform theorems [23]:

$$x(n - n_d) \leftrightarrow e^{-j\omega n_d} X(e^{-j\omega}) \quad (1)$$

where  $n_d$  is an integer, and  $X(e^{-j\omega})$  is the discrete Fourier transform of  $x(n)$ . However, we have:

$$|e^{-j\omega n_d} X(e^{-j\omega})| = |X(e^{-j\omega})| \quad (2)$$

Therefore, if we take an absolute value of the data in the frequency domain, then the shifting problem will be eliminated because:

$$|e^{-j\omega n_1} X(e^{-j\omega})| = |e^{-j\omega n_2} X(e^{-j\omega})| = |X(e^{-j\omega})| \quad (3)$$

where  $n_1$  and  $n_2$  are two different delay time periods due to two different detector shiftings.

In our experiments, we take an absolute value of each orientation (each column) of the raw GPR data and then take the inverse discrete Fourier transform (IDFT), i.e.,:

$$Y(i) = IDFT(|X(i)|), \quad i = 1, 2, \dots, 18 \quad (4)$$

where  $X(i)$  is the  $i$ th column of the raw GPR data which corresponds to the raw GPR data at the orientation of  $10i$  degrees, and  $Y(i)$  is the  $i$ th column of the output image. It should be noted that, by considering only the absolute values of data rather than the complex values, we lose the depth resolution by half due to symmetry.

### 3.1.3 Change Detection of GPR Signals from Adjacent Orientations

By assuming that the shifting problem is already corrected, the change detection can be easily achieved by signal subtraction. Consider the shift-corrected signals  $Y$ . We subtract the signal in the current orientation from the previous orientation, i.e.,:

$$Z(i) = Y(i+1) - Y(i), \quad i = 1, 2, \dots, 17 \quad (5)$$

where  $Z(i)$  is the  $i$ th column of the subtracted image which is the difference between the GPR signal in the orientation of  $10(i+1)$  degrees and that in the orientation of  $10i$  degrees. Therefore, we end up with 17 pairs of orientations. The subtracted GPR image (or change-detected image) of the GPR images of UXO and non-UXO shown in Figures 1 and 2 are depicted in Figures 6 and 7, respectively.

### 3.2 Energy-Based Features used in Detection

We compute the following features based on the GPR signal energy, the region of interest and the change detection image.

#### □ Maximum energy of GPR image $X$

We perform the maximum energy detection technique to represent a traditional technique. We use this maximum energy detection technique as a baseline in the comparison to our proposed technique. It is also used in our proposed technique as one of the features. The maximum energy of a given raw GPR image  $X$  in the frequency domain can be calculated by:

$$E_{\max} = \max_{i,j} |X(i, j)|^2 \quad (6)$$

#### □ Energy of the region of interest

Given  $X$  as a region of interest, the energy of the region of interest is computed by:

$$E_{ROI} = \sum_{i=1}^{Row} \sum_{j=1}^{Col} X^2(i, j) \quad (7)$$

where  $Row$  and  $Col$  are the number of rows and number of columns of  $X$ , respectively.

#### □ Maximum energy of the region of interest

Given  $X$  as a region of interest, the maximum energy of the region of interest is computed by:

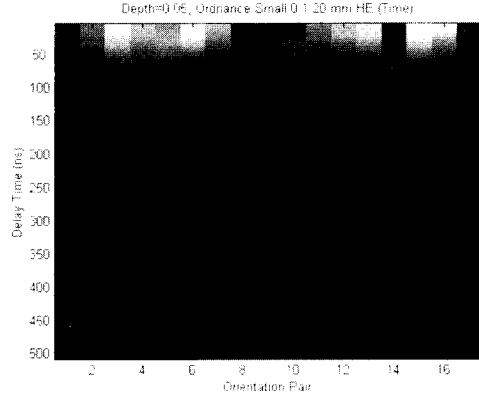


**Figure 6.** Time-domain subtracted GPR image of UXO corresponding to the frequency-domain GPR image show in Figure 1.

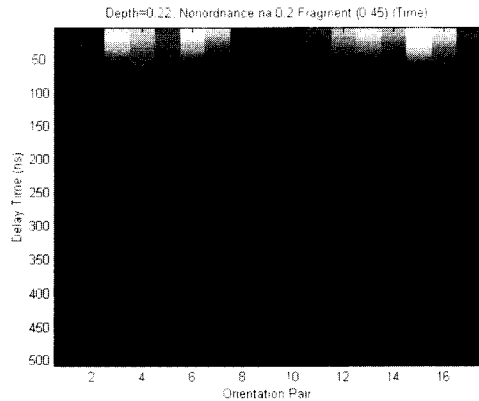


**Figure 7.** Time-domain subtracted GPR image of non-UXO corresponding to the frequency-domain GPR image show in Figure 2.

$$E_{\max, ROI} = \max_{i,j} X^2(i, j) \quad (8)$$

#### □ Energy of a change detection image

Given  $Z$  as a change detection image, its energy is computed by

$$E_{Change} = \sum_{i=1}^{Row} \sum_{j=1}^{Col} |Z(i, j)|^2 \quad (9)$$

where  $Row$  and  $Col$  are the number of rows and number of columns of  $Z$ , respectively.

### 3.3 Decision Rules

From the ground truth information that is provided along with this data set, we found that

most of non-UXO objects are of bigger size than UXO ones. We also set an assumption that a non-UXO object is of irregular shape. This assumption is intuitive because fragments in a battlefield are usually of random shapes. Therefore, the energy of object from the non-UXO class should be greater than that from the UXO class. The energy of the change detection GPR image described in section 3.2 should be small for an object with a regular shape like a UXO.

Hence, we set the decision rules of the energy detection technique and our proposed technique as the followings:

#### **Energy Detection (Baseline)**

*The object is UXO if  $E_{max} < TH1$ , otherwise it is Non-UXO.*

#### **Time-Domain Analysis (Proposed technique)**

*The object is UXO if  $E_{max} \times E_{ROI} \times E_{max,ROI} \times E_{Change} < TH2$ , otherwise it is Non-UXO.*

The thresholding values  $TH1$  and  $TH2$  are the parameters to be determined by an operator of a detection system on a clearance site. In our experiments,  $TH1$  and  $TH2$  are varied to several values to evaluate the detection performance of the techniques at several settings. We can see that the larger the value of thresholding, the more likely the object will be declared as a UXO.

## **4. Experimental Frameworks**

### **4.1 Evaluation Method**

The evaluation of a detection system is not straightforward. For example, the simplest way to detect all UXOs is to declare all objects in the data set as UXO. However, all non-UXOs will also be declared as UXO as well. In this case, the probability of stating "UXO" when a UXO is present or the probability of detection or true positives (TP) is 1. However, the probability of stating "UXO" when a non-UXO is present or the probability of false alarms or false positives (FP) is 1 as well. Therefore, the main goal is to achieve the largest TP with the smallest FP.

We evaluate our proposed technique and the energy detection technique in the form of a Receiver Operating Characteristic (ROC) curve which is a standard way to present overall

performance of a target detection system. A ROC curve is simply a plot of TP as a function of FP. It is created by varying the thresholding value and recording the numbers of correct and incorrect classifications at each value of thresholding. In this case, when the thresholding value  $TH$  is smaller, more images will be classified as non-UXO. If we would like to classify more UXOs correctly, then we will have to set  $TH$  to a larger value. However, many non-UXOs will be incorrectly classified as UXO as well. Therefore, a ROC curve can provide the system performance at any values of thresholding. We can also compare performances of detection systems by plotting their ROC curves. The ROC curve on the top-left has the better performance.

### **4.2 Experimental Results**

Figure 8 shows two ROC curves of a system based on energy detection and based on the proposed system variable on each day of the four-day data collection. In this section, we show the probability of detection or true positives (TP) from 0.5 to 1 because we would like to consider the system performance when it can classify at least half of UXOs correctly. We would not operate the system in the threshold range such that it can classify less than half of our targets correctly in a real-world application (in such a case, more than half of UXOs are classified as non-UXOs, which is dangerous.) We can see that the proposed technique outperforms the energy detection for most of the thresholding values.

The detection performances of the energy detection and the proposed technique on the entire data set are shown as ROC curves in Figure 9. It is clear that the proposed technique performs better than the energy detection technique for all of the thresholding values. In the figure, we also show the line of no discrimination ability, that is the plot when a system cannot tell the difference between UXO and non-UXO (TP=FP.) Therefore, we would like to have ROC curves of our techniques to be on the top-left of this line. As seen from Figure 9, both of the energy detection and the proposed technique have better performance than that.

For the UXO detection, missing a UXO is a serious problem. Therefore, it is desirable to have a TP of 1 because we would not like to miss any UXO. It can be seen from Figure 9

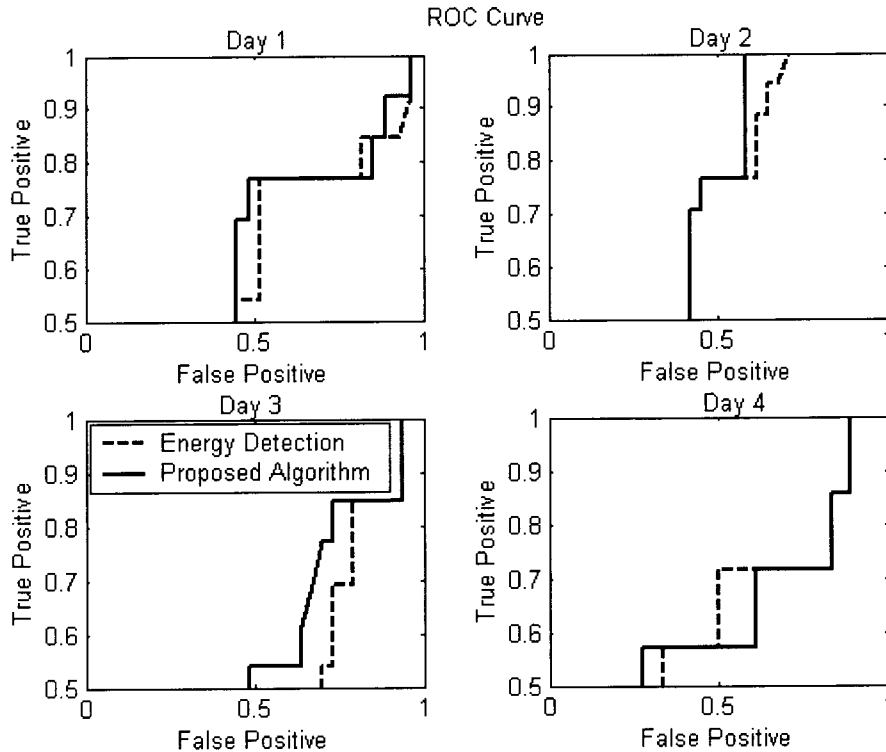


**Figure 8.** ROC curves of a system based on energy detection in contrast to that based on the proposed technique on each day of the data collection.

that, at the TP of 1, the proposed technique reduces the FP of 0.88 performed by the energy detection, to 0.84. In this particular data set, those percentages imply a reduction of the number of false alarms from 96 to 92. This means a detection system operator would not need to dig up 4 locations just to find non-UXOs. The false alarm reduction percentage in this case is  $(0.88 - 0.84) \times 100\% / 0.88 = 4.55\%$ . It should be noted that a graph in [3] by the U.S. Army Environmental Center and Naval Explosive Ordnance Disposal Technology Division indicates that the system of Battelle company (the system used to collect data in our experiments) achieved a TP of 0.47 with an FP of 0.53. It can be seen from Figure 9 that our proposed technique performs better by achieving a TP of 0.5 with an FP of about 0.4.

The results are even more interesting when we compare both techniques with the situation of no discrimination ability. In that case, the detection system operator has to make a decision by himself to clear the location by guessing

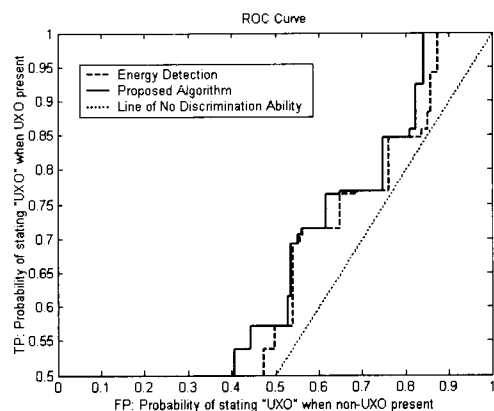


**Figure 9.** ROC curves of a system based on the energy detection in contrast to that based on the proposed technique on the entire data set.

or flipping a coin. In this data set, to get all UXOs or to accomplish a TP of 1, he has to dig up all 109 locations. Here, the number of false alarms reduction achieved by the proposed technique is 17 or  $(109 - 92) \times 100\% / 109 = 15.6\%$ ,

and the energy detection technique can reduce the false alarms by 11.9%.

## 5. Conclusion

Humanitarian demining has become an international issue nowadays. In this research we propose a new technique to analyze time-domain ground penetrating radar (GPR) signals of the UXO/non-UXO discrimination problem. The proposed technique is based on energy features of the region of interest and change detection. In our experiments, we use the GPR data set collected by Battelle company and the Ohio State University from the Jefferson Proving Ground (JPG), U.S.A. We also apply the energy detection technique to be the baseline of the experiments. The results in terms of Receiver Operating Characteristic (ROC) curves show that our proposed technique has better overall performance than the energy detection technique. Moreover, both of the techniques yield better results than the situation in which no technique is applied (no discrimination ability.) The reduction of false alarms by the proposed technique can save operations time and money in the UXO/land mine clearance.

## 6. Acknowledgments

The author would like to thank the Unexploded Ordnance Center of Excellence (UXOCOE), Department of Defense, U.S.A. for providing the data set. We acknowledge the contribution of Dr. James Keller, Dr. Paul Gader, Dr. Dominic Ho, and Dr. R. Joe Stanley through many technical discussions on UXO and land mine detection at the Computational Intelligence lab, MU.

## 7. References

- [1] C. King (Ed.), *Jane's Mine and Mine Clearance*, 2nd Ed., Biddles Ltd., 1997.
- [2] P. D. Gader, Pattern Recognition for Humanitarian De-Mining, *Proc. of the 16<sup>th</sup> Intl. Conf. on Pattern Recog.*, pp. 521–522, Quebec, Aug. 2002.
- [3] U.S. Army Environmental Center and Naval Explosive Ordnance Disposal Technology Division, *UXO Technology Demonstration Program at Jefferson Proving Ground*, Report No. SFIM-AEC-ET-CR-99051, May 1999.
- [4] Thailand Mine Action Center (TMAC), Available: <http://www.tmac.go.th>
- [5] H. Brunzell, Detection of Shallowly Buried Objects using Impulse Radar, *IEEE Trans. Geosci. Remote Sensing*, Vol. 37, pp. 875–886, Feb. 1999.
- [6] C. C. Chen and L. Peters, Jr., Buried Unexploded Ordnance Identification via Complex Natural Resonances, *IEEE Trans. on Antennas and Propagation*, Vol. 45, No. 11, pp. 1645–1654, Nov. 1997.
- [7] P. D. Gader, J. M. Keller, and B. N. Nelson, Recognition Technology for the Detection of Buried Land Mines, *IEEE Trans. on Fuzzy Systems*, Vol. 9, No. 1, pp. 31–43, Feb. 2001.
- [8] P. D. Gader, H. Frigui, B. Nelson, G. Vaillette, J. M. Keller, New Results in Fuzzy Set Based Detection of Landmines with GPR, *Proc. SPIE Conf. on Detection and Remediation Technologies for Mines and Minelike Targets IV.*, pp. 1075–1084, Orlando, FL, 1999.
- [9] P. D. Gader, B. Nelson, H. Frigui, G. Vaillette, J. M. Keller, Fuzzy Logic Detection of Landmines with Ground Penetrating Radar, *Signal Processing*, Vol. 80, No. 6, pp. 1069–1084, June 2000.
- [10] P. D. Gader, B. N. Nelson, A. Koksul Hocaoglu, S. Auephanwiriyaikul, M. A. Khabou, Neural versus Heuristic Development of Choquet Fuzzy Integral Fusion Algorithms for Land Mine Detection, *Neuro-Fuzzy Pattern Recognition*, World Scientific, Singapore, 2000.
- [11] P. D. Gader, M. Mystkowski, Y. Zhao, Application of Hidden Markov Models to Landmine Detection using Ground Penetrating Radar, *IEEE Trans. Geosci. Remote Sensing*, Vol. 39, pp. 1231–1244, June 2001.
- [12] K. C. Ho and P. D. Gader, Correlation Based Landmine Detection using GPR, *Proc. SPIE Conf. on Detection and Remediation Technologies for Mines and Minelike Targets V*, pp. 1088–1095, Orlando, FL, April 2000.
- [13] K. C. Ho and P. D. Gader, Improved Correlation Based Algorithm for Hand-Held Landmine Detector, *Proc. SPIE Conf. on Detection and Remediation Technologies for Mines and Minelike Targets VI*, pp. 483–493, Orlando, FL, 2001.

- [14] K. C. Ho and P. D. Gader, A Linear Prediction Land Mine Detector Algorithm for Hand Held Ground Penetrating Radar, *IEEE Trans. Geosci. Remote Sensing*, Vol. 40, No. 6, pp. 1374–1384, June 2002.
- [15] R. J. Stanley, N. Theera-Umpon, P. D. Gader, S. Homanchi, and D. K. Ho, Detecting Landmines using Weighted Density Distribution Function Features, *Proc. Of the SPIE Conf. on Signal Processing, Sensor Fusion, and Target Recognition X*, Vol. 4380, pp. 135–141, Orlando, Apr. 2001.
- [16] J. W. Brooks, M. W. Maier, and S. R. Vechinski, Applying System Identification and Neural Networks to the Efficient Discrimination of Unexploded Ordnance, *Proc. IEEE Conf. on Aerospace*, pp. 449–467, Aspen, CO, Feb. 1997.
- [17] N. Theera-Umpon, P. D. Gader, and D. K. Ho, Region-Based Time-Domain Processing of Hand-Held GPR, *UXO Countermining Forum*, New Orleans, Apr. 2001.
- [18] X. Xu, E. L. Miller, and G. Sower, A Statistical Approach to Multichannel Bline Signal Detection for Ground Penetrating Radar Arrays, *Proc IEEE Workshop on Sensor Array and Multichannel Signal Processing*, pp. 449–453, Cambridge, MA, March 2000.
- [19] W. J. Steinway, H. A. Duvoisin III, M. S. Tomassi, J. E. Thomas, G. Betts, C. Morris, B. Kahn, P. Stern, S. Krywick, K. Johnson, K. Dennis, W. Simoneaux, and B. Blood, Multi-Sensor Systems for Mine Detection, *Proc. IEEE Intl Conf. on Geoscience and Remote Sensing*, pp. 228–233, Seattle, WA, July 1998.
- [20] L. M. Collins, Y. Zhang, J. Li, H. Wang, L. Carin, S. J. Hart, S. L. Rose-Pehrsson, H. H. Nelson, and J. R. McDonald, A Comparison of the Performance of Statistical and Fuzzy Algorithms for Unexploded Ordnance Detection, *IEEE Trans. on Fuzzy Systems*, Vol. 9, No. 1, pp. 17–30, Feb. 2001.
- [21] R. J. Stanley, P. D. Gader and K. C. Ho, Feature and Decision Level Sensor Fusion of Electromagnetic Induction and Ground Penetrating Radar Sensors for Landmine Detection with Hand-Held Units, *Information Fusion*, Vol. 3, No. 3, pp. 215–223, 2002.
- [22] Battelle Company and Ohio State University ElectroScience Laboratory, *JPG IV Survey Data Analysis Report*.
- [23] A. V. Oppenheim and R. W. Schaffer, *Discrete-Time Signal Processing*, Prentice-Hall, 1989.